



ORIGINAL ARTICLE

Fabrication of tri-polymers composite film with high cyclic stability and rapid degradation for cardiac tissue engineering



Abdalla Abdal-hay^{a,b,*}, Hassan Fouad^c, Nasser M. Abd El-salam^c,
Khalil Abdelrazek Khalil^{d,e}

^a The University of Queensland, School of Dentistry, Herston, QLD 4006, Australia

^b Department of Mechanical Engineering, Faculty of Engineering, South Valley University, Qena 83523, Egypt

^c Applied Medical Science Department, Community College, King Saud University, P.O Box 10219, Riyadh 11433, Saudi Arabia

^d Department of Mechanical and Nuclear Engineering, College of Engineering, University of Sharjah, Sharjah 27272, United Arab Emirates

^e Department of Mechanical Engineering, King Saud University, P.O. Box 800, Riyadh 11421, Saudi Arabia

Received 18 March 2022; accepted 4 April 2022

Available online 9 April 2022

KEYWORDS

Cardiac Infraction;
Composite film;
Mechanical properties;
Silk fibroin;
Poly(lactide-co-ε-caprolactone);
Polyethylene oxide

Abstract In this communication, biodegradable and highly elastic silk fibroin/poly(lactide-co-ε-caprolactone)/polyethylene oxide (SF/PLCL/PEO) tri-polymers composite film was fabricated by sol-gel casting technology. The tri-polymers composite film exhibited a high cycle performance and rapid degradation rate by regulating the content of blending of the three polymer contents. The viability of cardiomyocyte cells was demonstrated for both SF/PLCL and SF/PLCL/PEO composite films after 1 day of culture, although the tri-polymers composite film demonstrated superior cell growth, attachment and spreading after culturing for 7 days. Study findings support the potential application of this biocompatible tri-polymers composite film as a heart patch substitute with multi-functionalities.

© 2022 The Author(s). Published by Elsevier B.V. on behalf of King Saud University. This is an open access article under the CC BY license (<http://creativecommons.org/licenses/by/4.0/>).

1. Introduction

Every year 17.9 million people worldwide, approximately 34 people every minute, lose their lives to cardiovascular disease (Ang et al., 2020; Sayed et al., 2019; Su et al., 2021b) Among those, severe damage of the myocardial tissue can occur by myocardial infarction. Myocardial infarction, commonly referred to as heart attack, is the sudden injury of part of the heart muscle due to loss of blood flow, resulting from blockage of one or more coronary arteries that supply blood and oxygen

* Corresponding author at: The University of Queensland, School of Dentistry, Herston, QLD 4006, Australia.

E-mail address: abdalla.ali@uq.edu.au (A. Abdal-hay).

Peer review under responsibility of King Saud University.



Production and hosting by Elsevier

to the heart. This already injured part of the heart risks being completely damaged without immediate intervention. Improving treatment strategies for cardiovascular diseases is a major challenge within the field of regenerative medicine (Kundu et al., 2014).

The wide array of regenerative medicine applications exacerbates the need for biocompatible materials with broad potential. Silk is an attractive natural polymer fulfilling most tissue engineering (TE) biomaterial requirements due to its excellent biocompatibility and low immunogenicity (Bae et al., 2020; Kundu et al., 2014; Su et al., 2021a). However, the degradation rate of this material is relatively low and uncontrollable during implantation. According to the U.S. Pharmacopeia, silk is a non-degradable biomaterial because it retains greater than 50% of its tensile integrity post-implantation. Moreover, silk fibroin (SF) casted film is brittle in nature, limiting its scope as a structural material.

As an FDA-approved biomaterial, there is clear evidence that protein silk is susceptible to proteolytic degradation and absorbed slowly *in vivo* (Altman et al., 2003; Asakura et al., 2021). As an implanted biomaterials' degradation rate should be considered in relation to the healing process (Cai et al., 2002a; Cai et al., 2002b), it appears vital to combine the characteristics of silk with another material that enables controlled degradation.

Regarding our hypothesis, it has been reported that the silkworm *Bombyx mori* produces a protease inhibitor in the silk gland, embedding it within the silk cocoon for protection against premature proteolytic degradation (Cai et al., 2002b). Incorporating fast biodegradable polymers causes conformational changes in the protein structure, potentially increasing susceptibility to degradation (Cai et al., 2002a, 2002b; Wang et al., 2008, 2007). Thus, blending of SF based biomaterials with fast degradable polyethylene oxide (PEO) as a water-soluble polymer, (Li et al., 2005) and poly(lactide-co- ϵ -caprolactone) (PLCL) as a highly elastic (break elongation of about 300%) (Sun et al., 2016) material, can accelerate the degradability and enhance the fatigue properties of the composite film. Therefore, we aimed to develop a new bio-composite polymer from the synthetic polymers PEO and PLCL, and protein polymers, by inexpensive and straightforward sol-gel casting technology to accelerate the degradation rate and enhance the fatigue properties of SF. In addition, the proposed composite film with high cyclic stability, rapid degradability and good cytocompatibility can provide greater insight into the appropriate SF-based biomaterials scaffold design for cardiac TE applications.

2. Materials and methods

According to previously published work, the extraction procedure of B. Mori silk fibroin is shown in the schematic diagram of Fig. 1a (1–4). *Cocoons of B. Mori silkworm* (Amazon, Item Model Number: 1838RNZ5522WWU6R) were boiled for 30 min in an aqueous solution of 0.02 M Na₂CO₃, then rinsed thoroughly with warm water to extract the glue-like sericin proteins. The dialysed aqueous silk solution was then lyophilised for three days and left to dry at room temperature. The three lyophilised materials SF, PEO granular (average molecular weight of 6×10^5 , Aldrich) and PLCL irregular particles (PLCL, Mw = 300 kDa, LA: CL = 50:50, Jinan Daigang

CO. Ltd, China), in a 2.0 wt%, were dissolved separately in formic acid: acetic acid ratio of 3:1 by volume. Blends of SF/PLCL (1:2) and SF/PLCL/PEO (1:2:1) in a volume ratio were prepared by adding each polymer solution dropwise directly into the other and stirring vigorously at ~ 40 °C for 1.0 h. Finally, 90 ml of the blends solution was cast into 25 cm glass-Petri dishes plates and left to dry in a fume hood at 25 °C for 72 h, and then under vacuum for an additional 24 h (Fig. 1a (5–7)). A thin film of less than 150 μ m thickness was formed.

The surface morphology of the prepared films was imaged by scanning electron microscopy (SEM, Joel 7001F, Japan) after sputter-coated with a 10 nm layer of platinum. Fourier transforms infrared (FTIR) spectra (a Bruck EQUINOX55) in the wavelength range between 4000 and 400 cm^{-1} in transmittance mode was used to evaluate the film. Thermal analysis using TGA/DSC ((DSC; NETZSCH DSC 200PC) at a heating rate of 10 °C/min was used to assess the films' chemical composition and thermal characteristics. A cyclic test (BioTester 5000, CellScale, Canada) was performed at 25 °C with a loading rate of 10 mm min^{-1} . Samples were stretched and relaxed toward the original length, repeatedly undergoing 10% of the total strain. Loading-unloading cycles were plotted in terms of stress-strain in 10 cycles. 0.1 mol/l of Tris was used as a buffer solution with free inorganic components to investigate the degradation performance of the fabricated composite films (5 mm diameter size) at 37 °C for 7 and 60 days under 40 rpm continuous shaking. The weight loss of the dry composite film before and after immersion was calculated. Each test (mechanical tests and weight loss) was performed five times. Finally, SEM observed the surface morphology of the immersed films.

Cell Culture: According to the previous publication (Engel et al., 1999), a cell culture test was performed using cardiomyocytes cells that were isolated from 3-days Sague Dawley rats. Further experimental details including cells isolation procedures, incubation, cell viability (live/dead assay), metabolic activities (MTT assay) and cells morphology are shown in [supporting information](#).

Statistical analysis: GraphPad Prism (v.7.0, GraphPad Software, Inc., San Diego, CA, USA) was used for statistical analysis, applying one-way ANOVA and Tukey's multiple comparison tests. A p value < 0.05 was considered statistically significant.

3. Results and discussion

The present study demonstrated that casted pure SF film (SF only) in the dry phase was very brittle and unsuitable for practical use. As such, pure SF was not included in this study. However, these limitations might be improved by blending with PEO or PLCL polymers. The top surface morphologies of the solo and composite films obtained from SEM images are shown in Fig. 1b, with both solo and composite films exhibiting a solid, dense structure.

Interestingly, SEM of SF/PLCL composite film did not show a phase separation, while SF/PLCL/PEO composite film showed irregular surface characteristics and micro-phase separation. In addition, the surface characteristics of SF/PLCL/PEO blends showed the roughest properties due to microphase separation. In the case of the silk fibroin/PEO (98/02 wt%) blend,

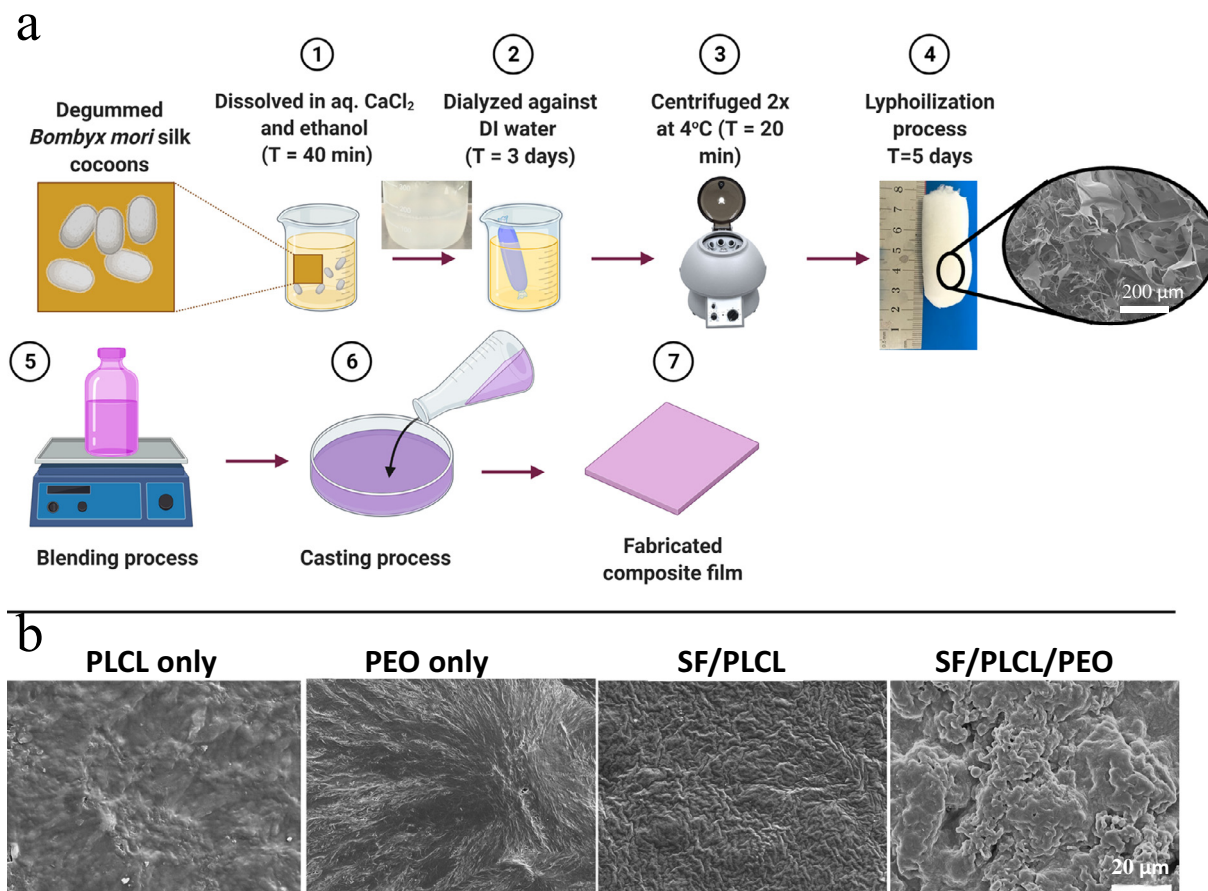


Fig. 1 (a) Illustrates the schematic diagram of SF preparation (1–4) and fabrication processes of composite films (5–7); (b) SEM images illustrate the top surface of solo and composite fabricated films.

an evenly dispersed micro-size PEO phase was observed. The PEO can be easily extracted from the film with water to generate SF/PLCL composite matrices with definable porosity and enhanced surface roughness. Our findings also suggest that the poor miscibility of SF/PLCL/PEO composite polymers might provide potential rapid leaching out of PEO molecules during degradation, as discussed later.

ATR-FTIR spectroscopy studied the intermolecular interactions and compatibility of PLCL, PEO, and SF in the fabricated composite films (Fig. 2a). Films were also analysed using ATR-FTIR to ensure that PLCL or/and PEO were successfully incorporated into the composite matrix. To compare the interactions between PLCL, PEO, and SF in composite films, a spectrum for the extracted SF was created, as shown in Fig. 3a, where an expanded 2000–750 cm⁻¹ selected area of the ATR-FTIR spectra was reproduced for higher resolution. Major absorption bands assigned to amide-II (C-single bond-N stretching and N-single bond-H in-plane bending vibrations), amide-I (C=O stretching) and amide-A, (N-single bond-H stretching) for extracted SF can be seen at 1513, 1618, and 3278 cm⁻¹, respectively [8]. Sharp and symmetrical H-bonded N-single bond-H absorption band at the 3278 cm⁻¹ presented in SF is slightly shifted to the right in composites.

A slight shift can also be seen in the amide-II and amide-I areas, with new bands appearing about 1630 and 1523 cm⁻¹. These findings demonstrate relatively strong hydrogen bond-

ing or dipole–dipole type intermolecular interactions between the ester and amide groups (Nazeer et al., 2019) in PLCL and SF, resulting in good compatibility between the two polymers. Characteristic, mighty –CH₂ stretching peak for PLCL is also present at around 2942 and 1757 cm⁻¹ in PLCL only and SF/PLCL composites (Sun et al., 2016). The presence of SF amide bands alongside PLCL characteristics bands, such as C=O stretching (1723 cm⁻¹), CH₂ stretching (2943 and 2865 cm⁻¹), and C-single bond-O stretching (1294 cm⁻¹), indicates that PLCL molecules were successfully incorporated into the SF matrix in composite films (Sun et al., 2016). These findings are consistent with those previously reported (Singh et al., 2020). In addition, the strong chemical interactions bond might enhance mechanical properties such as tensile strength and cyclic loading of the composite films (Sun et al., 2016). However, the PEO did not show a distinct characteristic absorption band in the amide I and amide II regions of SF in the composite film, indicating a negligible effect on the molecular structural properties. This absence of interaction between PEO molecules and the SF/PLCL matrix might remove and sacrifice the PEO from the composite films and create a porous structure during the degradation process, subsequently accelerating the films' degradation rate without dramatic damage to the composite scaffold (Jin et al., 2004).

The TGA and DSC curves of plain and composite films indicated differences in their thermal behaviour, as shown in Fig. 2c and d. The results demonstrated that incorporating

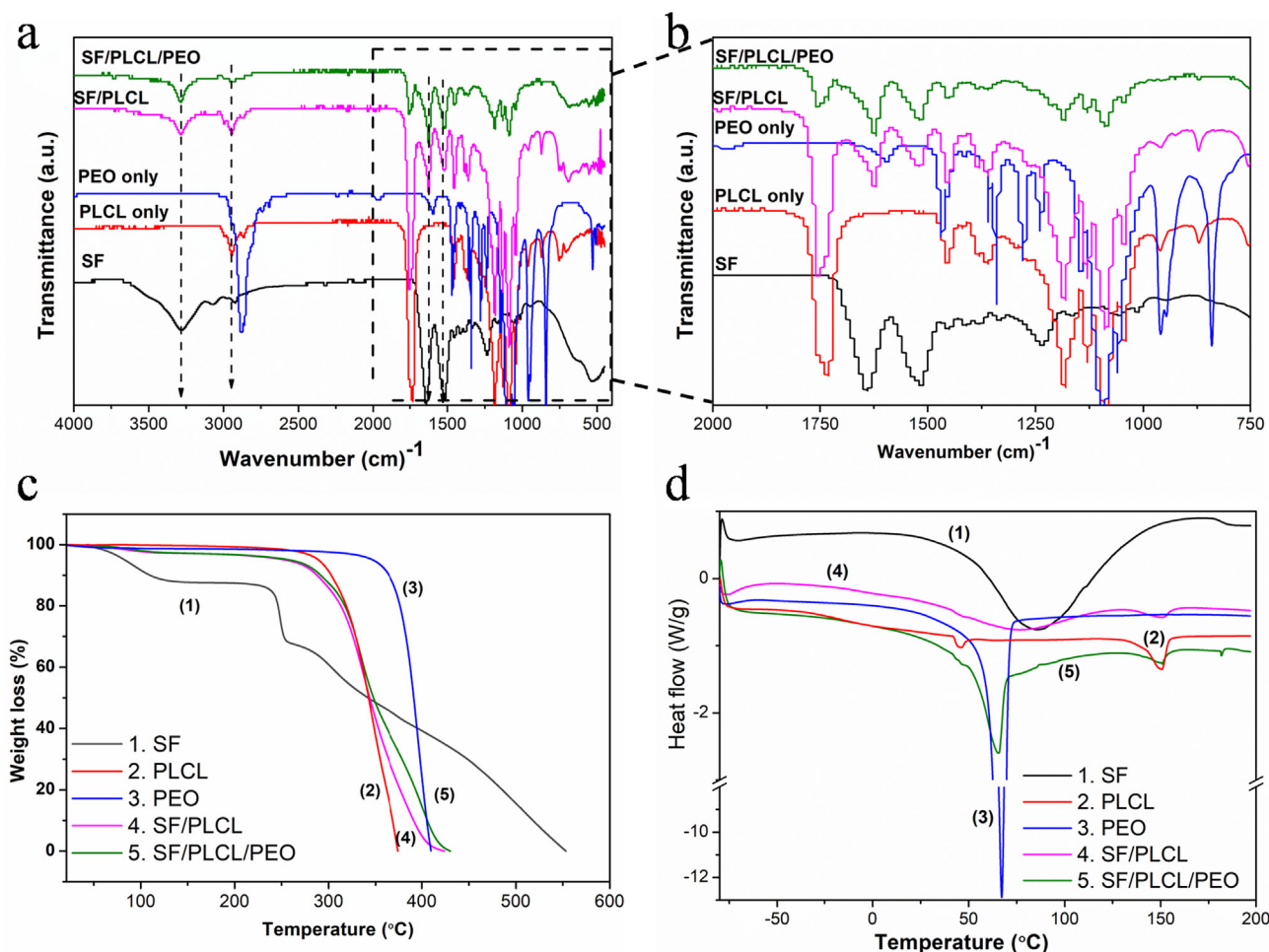


Fig. 2 (a and b) FTIR at 400–4000 and 750–2000 cm^{-1} wavenumbers, respectively; (c) TGA and (d) DSC thermal analysis of fabricated pure and composite films.

both PLCL and PEO enhances the thermal properties of composite films. TGA data indicated the similar thermal characteristics of SF to the previous reports of fabricated pure SF (Chen et al., 2012). The pure SF film presented an initial weight loss below 100 °C due to the presence of moisture, and, as the temperature is increased, the second weight loss induced an abrupt decrease at above 223 °C (Fig. 2c). Because SF possesses a more complex protein structure, the pyrolysis (complete decomposition) process was completed at 550 °C. This could be attributed to the slow thermal decomposition nature of natural polymers compared to synthetic polymers (Chen et al., 2012). There was no significant weight loss of pure PLCL, PEO and composite films when the temperature increased from 25 °C to their decomposition temperatures (Fig. 2c). The decomposition of PLCL occurred at ~ 310 °C due to polymer pyrolysis, and the residual weight approached zero at about 385 °C, as typically observed for a synthetic polymer (Chen et al., 2015). PEO film had the highest decomposition temperature (~ 395 °C) and entirely decomposed at 423 °C. The starting decomposition temperatures and complete weight loss temperatures of SF/PLCL and SF/PLCL/PEO composite films were similar at ~ 283 °C and 443 °C, respectively.

DSC analysis is used to investigate compatibility of a blend. Most importantly, the DSC curves of composite films showed

the broad endothermic peaks corresponding to SF, confirming the blending of PCL and PEO with SF (Fig. 2d). The broad temperature endothermic peak of pure SF centred at ~ 86.44 °C (total enthalpy 298.4 J g^{-1}) is commonly reported (Motta et al., 2002; Wang and Zhang 2013). However, in the present study, this broad peak of pure SF was shifted to a lower value at ~ 73.57 °C with total enthalpy of 68.11 J g^{-1} in SF/PLCL composite film. This shifting is likely due to the interfacial bonding between the SF and PCL molecules in the composite films (Chen et al., 2015), indicating fair compatibility between the two polymers in the SF/PLCL composite film (Singh et al., 2020).

Since cardiovascular is a motorial tissue accompanying various motions, the mechanical behaviour investigation of the heart patch is required to ensure its daily activities. It was found in the cyclic mechanical tests that there is an obvious hysteresis loop for the first cycle curves in composite films (Fig. 3a). The mechanical properties of the films, however, do not change significantly from the second to the tenth cycle, with overlapping of nearly all curves from the second to the following cycles, as shown in Fig. 3b. For all the cycle curves, the unloading region, including the first cycle, were nearly identical, indicating that the energy stored in each cycle was unchanged (Liu et al., 2022). Although the apparent hysteresis

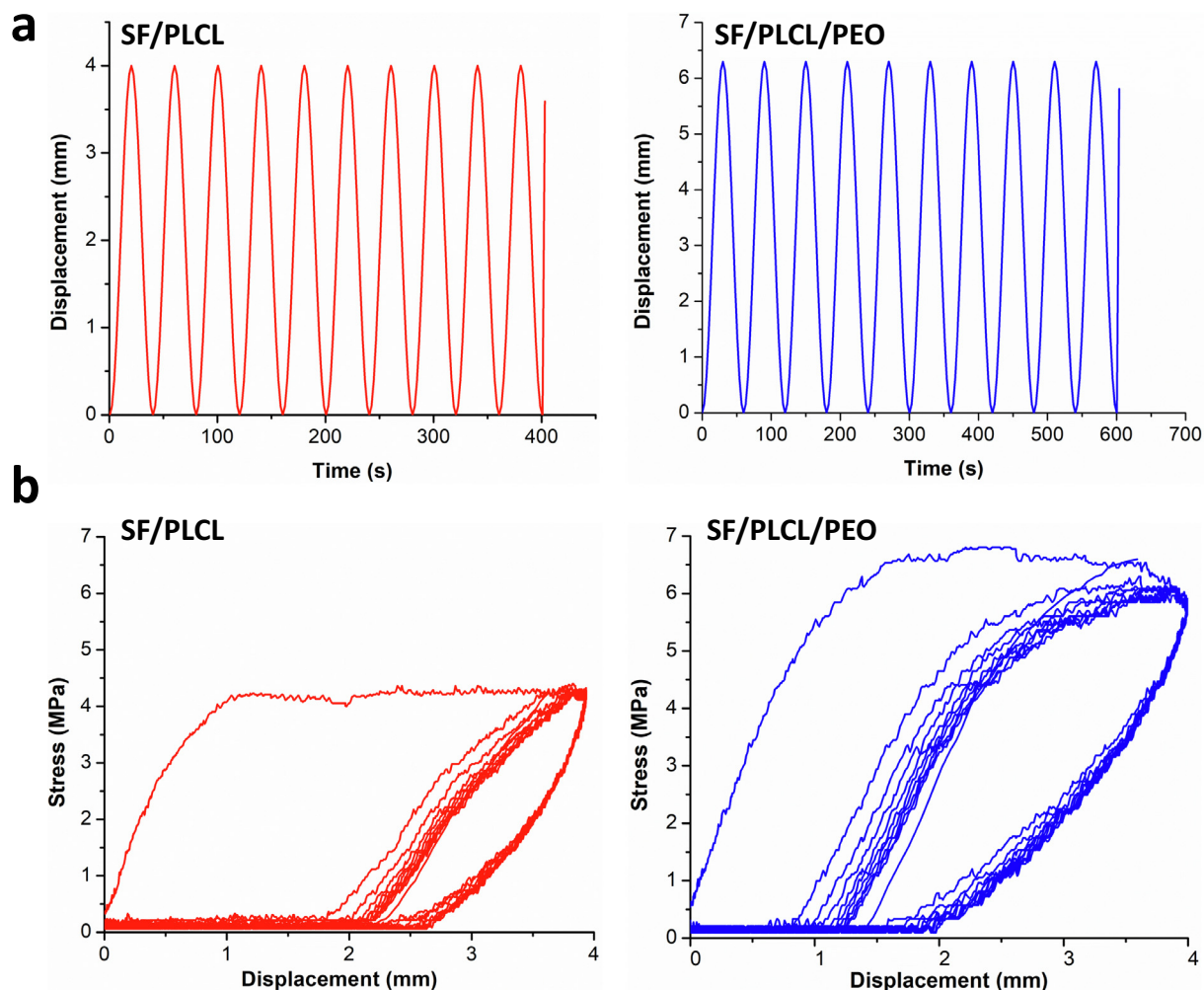


Fig. 3 (a) Behaviour of the composite films under cyclic loading and (b) loading–unloading curves of the composite films with a sinusoidal wave at 10% strain.

loops are observed in bi- and tri- polymer composite films, the hysteresis loop of SF/PLCL/PEO composite film is the largest. It indicates that the introduction of PEO could make the tri-polymers composite films dissipate energy more efficiently than the SF/PLCL one, causing excellent mechanical properties such as extensibility and toughness (Abdal-Hay et al., 2018). These excellent mechanical properties make our developed composite films a promising candidate for TE application.

The SF/PLCL/PEO tri-polymers composite film showed higher weight loss after immersion for 7 and 60 days than SF/PLCL composite films by approximately 4.8 ± 0.85 wt% and 15.3 ± 3.2 wt%, respectively. This is likely due to the leaching of PEO molecules from the SF/PLCL/PEO composite films, as shown from the surface morphology after 60 days of degradation (Fig. 4a) (Sayed et al., 2019). However, leaching out of PEO creates a porous morphology not observed in the neat samples (Fig. 1b). The induced porous structure might impact the degradation of the composite films via physiological penetration during implantation. It has been reported that morphological parameters (e.g., porosity, pore size, thickness,

surface-area-to-volume ratio) have an evident impact on the degradation performance of SF molecules (Kundu et al., 2014; Mousa et al., 2020). The tensile properties of the SF/PLCL composite scaffold did not show significant changes compared to the SF/PLCL/PEO film after immersion for 60 days as depicted in Fig. 4b. However, tensile stress–strain curves of composite films before and after immersion pursue similarly.

The live/dead assay was employed to determine the cell viability of the fabricated SF/PLCL and SF/PLCL/PEO composite films after one day of cell culture. The two examined composite films showed no toxicity on cells, at least for the indicated period of one day. Laser confocal microscopy images of live/dead staining showed higher cell viability (Fig. 5a) and proliferation (live cells, green) for the composite film without PEO than the one containing PEO (Fig. 5b). This is likely due to the presence of PEO molecules on the surface that might, with low protein adsorption, hinder cell proliferation at the early time point (Li et al., 2005). However, both composite films observed minimum dead cell (red) staining, demonstrating high *in vitro* viability of cells by the composite films

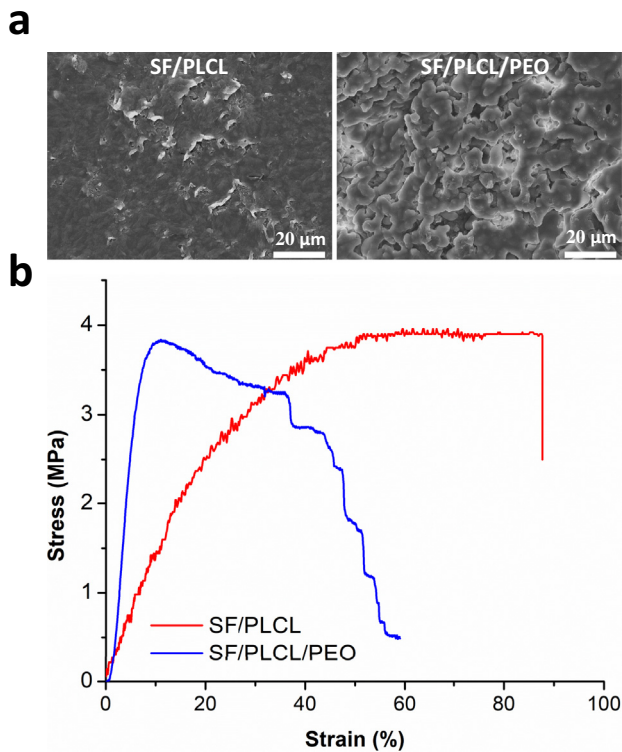


Fig. 4 (a) SEM images and (b) Tensile stress–strain curves of composite films after immersion in a Tris-HCl buffer solution for 60 days at 37 °C. The tensile test was conducted using the same sample size and under the same test parameter conditions as the fatigue test.

throughout the culture. The colorimetric MTT assay was used as an established method for evaluating cell proliferation on the fabricated scaffolds after 7 days to further investigate the effects of PEO over an extended culture period (Fig. 5d). Assay results demonstrated that as the culture time is extended, better growth and proliferation occur on tri-polymers composite film (SF/PLCL/PEO) compared to SF/PLCL film. After 7 days of cell culture, the tri-polymers composite film significantly showed higher cell growth and proliferation than SF/PLCL composite film. This might contribute to the leaching of PEO molecules from the composite surface observed at the same culture time point (Fig. 5e). These results align with cell spreading and attachment observed with SEM after 7 days of culture (Fig. 5c and d), which indicated that leaching out of PEO from the tri-polymers composite film increases the surface area (due to establishing porous structure) and surface roughness, and subsequently enhances cell attachment, spreading and proliferation.

4. Conclusion

Solution blending was employed to incorporate water-soluble PEO and superelastic PLCL into SF to enhance degradation and mechanical properties. Due to strong interfacial bonding between the polymer molecules, specifically between PLCL and SF, the thermal stability and cycling loading were dramati-

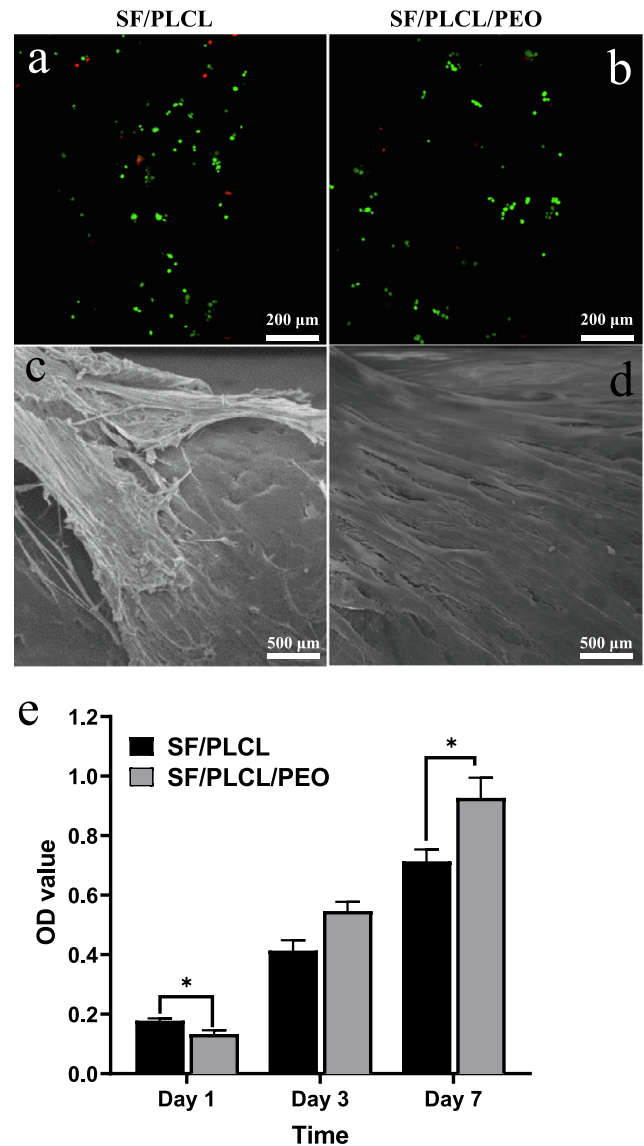


Fig. 5 Illustrates (a and b) cytotoxicity (cell viability) assessed by live/dead assay (green staining shows live cells and red staining presents dead cells) after 1 day of cardiomyocytes cells culture; (c and d) SEM images of cardiomyocytes cells attachment and spreading after 7 days of culture; and (e) MTT metabolic assay after 1, 3 and 7 days of cardiomyocytes culture.

ically improved. The biocompatibility of SF/PLCL/PEO composite film was demonstrated by supporting the growth of cardiomyocytes *in vitro*. The combination of these characteristics, together with a cost-effective and straightforward preparation method, demonstrates the potential of this tri-polymers film in developing a heart patch substitute material, and more globally, towards the production of high-performance 3D biomaterials scaffolds for TE application.

Acknowledgement

This project was funded by the National Plan for Science, Technology and Innovation (MAARIFAH), King Abdulaziz City for Science and Technology, Kingdom of Saudi Arabia, Award Number (15-BIO4042-02).

Appendix A. Supplementary material

Supplementary data to this article can be found online at <https://doi.org/10.1016/j.arabjc.2022.103902>.

References

- Abdal-Hay, A. et al, 2018. Electrospun biphasic tubular scaffold with enhanced mechanical properties for vascular tissue engineering. *Mater. Sci. Eng. C Mater. Biol. Appl.* 82, 10–18.
- Altman, G.H. et al, 2003. Silk-based biomaterials. *Biomaterials* 24 (3), 401–416.
- Ang, S.L. et al, 2020. Potential applications of polyhydroxyalkanoates as a biomaterial for the aging population. *Polym. Degrad. Stab.* 181, 109371.
- Asakura, T. et al, 2021. Structure and dynamics of biodegradable polyurethane-silk fibroin composite materials in the dry and hydrated states studied using ¹³C solid-state NMR spectroscopy. *Polym. Degrad. Stab.* 190, 109645.
- Bae, B.B., Kim, M.H., Park, W.H., 2020. Electrospinning and dual crosslinking of water-soluble silk fibroin modified with glycidyl methacrylate. *Polym. Degrad. Stab.* 179, 109304.
- Cai, K. et al, 2002a. Influence of different surface modification treatments on poly(D, L-lactic acid) with silk fibroin and their effects on the culture of osteoblast in vitro. *Biomaterials* 23 (7), 1603–1611.
- Cai, K. et al, 2002b. Poly (D, L-lactic acid) surfaces modified by silk fibroin: effects on the culture of osteoblast in vitro. *Biomaterials* 23 (4), 1153–1160.
- Chen, C.-H. et al, 2015. Dual functional core–sheath electrospun hyaluronic acid/polycaprolactone nanofibrous membranes embedded with silver nanoparticles for prevention of peritendinous adhesion. *Acta Biomater.* 26, 225–235.
- Chen, J.-P., Chen, S.-H., Lai, G.-J., 2012. Preparation and characterization of biomimetic silk fibroin/chitosan composite nanofibers by electrospinning for osteoblasts culture. *Nanoscale Res. Lett.* 7 (1), 1–11.
- Engel, F.B. et al, 1999. A mammalian myocardial cell-free system to study cell cycle reentry in terminally differentiated cardiomyocytes. *Circ. Res.* 85 (3), 294–301.
- Jin, H.-J. et al, 2004. Human bone marrow stromal cell responses on electrospun silk fibroin mats. *Biomaterials* 25 (6), 1039–1047.
- Kundu, B. et al, 2014. Silk proteins for biomedical applications: bioengineering perspectives. *Prog. Polym. Sci.* 39 (2), 251–267.
- Li, C.M. et al, 2005. Silk apatite composites from electrospun fibers. *J. Mater. Res.* 20 (12), 3374–3384.
- Liu, B. et al, 2022. Simultaneous biomechanical and biochemical monitoring for self-powered breath analysis. *ACS Appl. Mater. Interf.* 14 (5), 7301–7310.
- Motta, A., Fambri, L., Migliaresi, C., 2002. Regenerated silk fibroin films: thermal and dynamic mechanical analysis. *Macromole. Chem. Phys.* 203 (10–11), 1658–1665.
- Mousa, H.M. et al, 2020. Development of biocompatible tri-layered nanofibers patches with endothelial cells for cardiac tissue engineering. *Euro. Polym. J.* 129, 109630.
- Nazeer, M.A., Yilgor, E., Yilgor, I., 2019. Electrospun polycaprolactone/silk fibroin nanofibrous bioactive scaffolds for tissue engineering applications. *Polymer* 168, 86–94.
- Sayed, M.M. et al, 2019. Enhancing mechanical and biodegradation properties of polyvinyl alcohol/silk fibroin nanofibers composite patches for Cardiac Tissue Engineering. *Mater. Lett.* 255, 126510.
- Singh, R. et al, 2020. Optimization of cell seeding on electrospun PCL-silk fibroin scaffolds. *Euro. Polym. J.* 134, 109838.
- Su, Y. et al, 2021a. Muscle fibers inspired high-performance piezoelectric textiles for wearable physiological monitoring. *Adv. Funct. Mater.* 31 (19), 2010962.
- Su, Y. et al, 2021b. Self-powered respiration monitoring enabled by a triboelectric nanogenerator. *Adv. Mater.* 33 (35), 2101262.
- Sun, B. et al, 2016. Polypyrrole-coated poly (l-lactic acid-co-ε-caprolactone)/silk fibroin nanofibrous membranes promoting neural cell proliferation and differentiation with electrical stimulation. *J. Mater. Chem. B* 4 (41), 6670–6679.
- Wang, H.-Y., Zhang, Y.-Q., 2013. Effect of regeneration of liquid silk fibroin on its structure and characterization. *Soft Matter* 9 (1), 138–145.
- Wang, X. et al, 2008. Controlled release from multilayer silk biomaterial coatings to modulate vascular cell responses. *Biomaterials* 29 (7), 894–903.
- Wang, X. et al, 2007. Silk coatings on PLGA and alginate microspheres for protein delivery. *Biomaterials* 28 (28), 4161–4169.